High-Field Nb_3Sn Cos-theta Dipole with Stress Management

Igor Novitski, Justin Carmichael, Vadim V. Kashikhin, and Alexander V. Zlobin

***Abstract*— Cost-effective superconducting dipole magnets with operating fields up to 16 T are being considered for the LHC energy upgrade (HE-LHC) and a Future Circular Collider (FCC). To demonstrate feasibility of 15 T accelerator quality dipole magnets, FNAL as a part of the US-MDP is developing a single-aperture Nb3Sn dipole demonstrator based on a 4-layer graded cos-theta coil with 60 mm aperture and cold iron yoke. In parallel, to explore the limit of the Nb3Sn accelerator magnet technology, optimize magnet design and performance parameters, and reduce magnet cost, magnet design studies are also being performed to push the nominal bore field to 16 T in a 60-mm aperture cos-theta dipole. Results of these studies are reported and discussed in this paper.**

***Index Terms*— Accelerator magnet, magnetic field, mechanical structure, Nb3Sn Rutherford cable, stress management.**

I. Introduction

ACCELERATOR MAGNET technology based on the Nb_3Sn superconductor has demonstrated a significant progress during the past decade [1]. Based on that, the Nb_3Sn dipoles and quadrupoles with a nominal field of 11-12 T are being developed for the LHC luminosity upgrade (HL-LHC project) [2] in the near future. In the longer term, the cost-effective 15-16 T Nb_3Sn magnets will be needed for the LHC energy upgrade (HE-LHC) or a future Very High Energy *pp* Collider (VHE*pp*C) [3].

To demonstrate the feasibility of accelerator quality 15 T dipole magnets, FNAL in collaboration with other members of the U.S. Magnet Development Program (MDP) is developing a 15 T Nb_3Sn dipole demonstrator based on a 4-layer graded cos-theta coil with a single 60-mm aperture and a 600-mm diameter cold iron yoke [4].

In parallel, magnet design studies are being conducted to explore the limits of the Nb_3Sn accelerator magnet technology and pushing the nominal bore field to 16 T in a 60-mm aperture cos-theta dipole. A preliminary analysis indicated that such a goal could not be achieved without stress management (SM) inside the coil [5]. The results of these studies, including a possible stress management technique are discussed below and compared with the baseline (BL) 15 T dipole demonstrator parameters.

II. Magnet Design

The magnetic and mechanical designs for the 15-T dipole demonstrator have been reported elsewhere [4]. The BL design analysis has shown that the main limitation for achieving higher fields are related to unloading of the inner layer pole under Lorentz forces and a separation of the pole turn from the pole block at the fields above 15 T. The natural step to solve this problem would be to increase the coil preload. However, that possibility has already been exhausted in the BL design as the equivalent stress in the coil midplane already approached to 180 MPa, which is close to the limit for the brittle Nb_3Sn conductor.

A. Stress management concept

To overcome these limitations, the following strategy was developed:

- keep the traditional shell-type structure with the floating wedges and pole blocks for the inner coil (layers 1and 2);
- maximally unload the inner coil by redistributing turns between the inner and the outer coil;
- introduce the azimuthal and radial SM in the outer coil (layers 3 and 4) only.

This approach builds upon the SM concept first proposed for the high-field Nb_3Sn block-type coils [6] and recently used in the canted-cos-theta magnets [7]. It also allows decoupling the fine tuning of the field quality (which is more sensitive to the inner coil geometry) from the SM optimization. In addition, it would later allow testing the new outer SM coils together with the inner BL coils (even though such configuration is not optimal) to save on the fabrication time and R&D cost.

B. Strand and cable

Similar to the BL design, the SM design has graded coil based on two Rutherford cables. Both cables are 15.1 mm wide, have a keystoned cross-section with the keystone angle of 0.805 degree, and use the Nb_3Sn strands with a Cu/nonCu ratio of 1.13 and Jc at 15 T, 4.2 K of 1500 A/mm^2. The inner cable has 28 strands, each 1 mm in diameter, and the outer cable has 40 strands, each 0,7 mm in diameter. The cable mid-thickness is 1.870 mm and 1.319 mm for the inner and outer cable respectively.

C. Coil design with stress management

As it was mentioned above, the inner 2-layer coil has three winding blocks separated by two wedges in layer 1 and two winding blocks and one wedge in layer 2 similar to the BL inner coil.

Each layer of the outer coil was split into 5 blocks, with the number of turns approximately following the cos-theta distribu-

This work is supported by Fermi Research Alliance, LLC, under contract No. DE-AC02-07CH11359 with the U.S. Department of Energy

Authors are with the Fermi National Accelerator Laboratory (FNAL), Batavia, IL 80510 USA (e-mail: zlobin@fnal.gov).

tion and the equal 5-mm spacing between the blocks. In addition, the outer coil layers were separated by 5 mm in the radial direction from each other and from the inner coil to create space for the support structure.

The inner coil was optimized for the best field quality using ROXIE code [8] considering the field harmonics produced by the outer coil. The model included a cylindrical iron yoke with the outer diameter of 600 mm and non-linear magnetic properties. The SM coil cross-section is shown in Fig. 1.

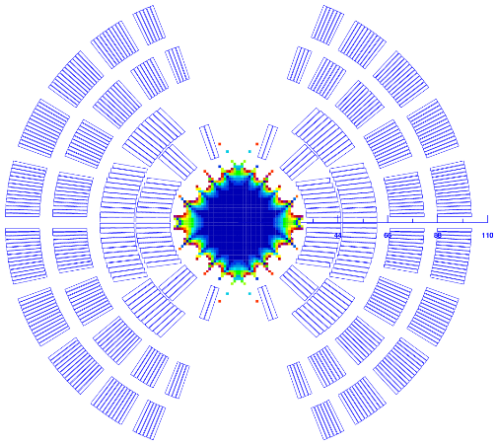

Fig. 1. Cross-section of SM coil with field uniformity diagram (dB/B1<2×10^{-4}).

D. Coil mechanical structure

Fig. 2 shows layer 3 of the outer-coil wound into the coil support structure. The structure is made of stamped stainless steel laminations providing precise and reproducible coil geometry. Coil ends include a support tube with special profile to provide turn alignment on the layer OD, end spacers and saddles. The end geometry of layer 3 of the outer coil is shown in Fig. 3.

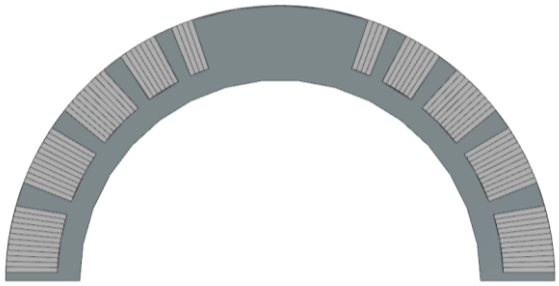

Fig. 2. The cross-section of layer 3 of the outer coil.

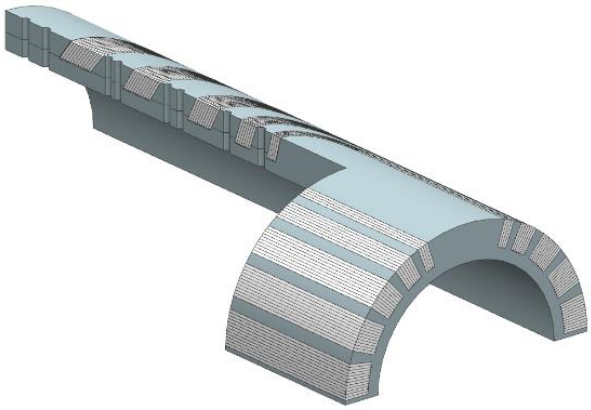

Fig. 3. The end geometry of layer 3 of the outer coil.

III. Magnetic Analysis

A. Magnet parameters

The main magnet parameters are summarized in Table 1. Since the SM design has 30% more turns than the 15 T dipole demonstrator [4], it reaches a higher field at a lower current, and consequently has a larger inductance and stored energy. Due to the smaller number of turns in the IL coil, the horizontal Lorentz force per the inner coil in the SM design is a factor of 1.2 smaller and the vertical force is a factor of 2.4 smaller than in the 15 T dipole demonstrator design. However, the horizontal force on the outer SM coil is a factor of 3 higher than that for the outer coil of the 15 T dipole demonstrator, while the vertical force is practically the same. This additional horizontal force is intercepted with a special support structure described above.

TABLE I
MAGNET PARAMETERS AT SSL AND 4.2 K

Parameter	SM	
	IC	OC
Bore field, T	16.07	
Peak field, T	16.44	
Current, A	10.80	
Inductance, mH/m	35.42	
Stored energy, MJ/m	2.06	
F_x, MN/m/quadrant	4.8	4.7
F_y, MN/m/quadrant	-0.5	-3.6
Number of turns	38	102

B. Short sample limit

Sensitivity of the magnet bore field to the operation temperature and the superconductor critical current density is shown in Fig. 3. For the nominal J_c(15T,4.2K) of 1500 A/mm^2 (which is close to 3000 A/mm^2 at 12 T, 4.2 K), the SM design reaches 16.1 T and 17.6 T fields at 4.2 K and 1.9 K respectively. Considering 16 T as the nominal field for the operation at 1.9 K, the critical current margin of 10% is provided using the state-of-the-art Nb_3Sn wires.

The bore quench field varies by about 0.5 T for every 500 A/mm^2 change in the critical current density. To consider 17 T as the nominal field at 1.9 K, the strand critical current density should be increased to 4000 A/mm^2 at 12 T and 4.2 K.

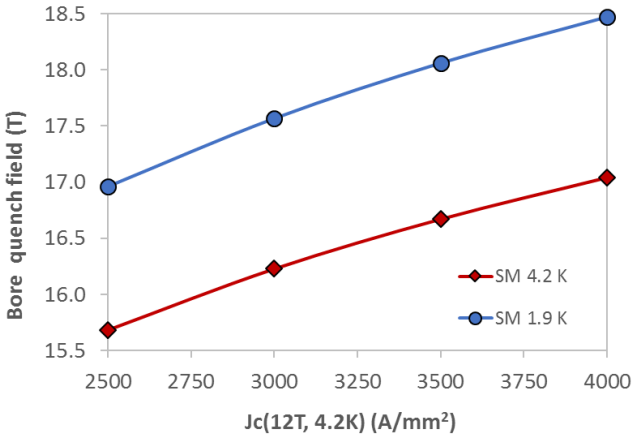

Fig. 3. The maximum bore field vs. the Nb_3Sn wire J_c at 12 T and 4.2 K.

C. *Field quality*

The calculated geometrical field harmonics are shown in Table 2. In the optimized SM coil the normalized harmonics values are smaller than 10^{-4} at the reference radius of 17 mm.

TABLE II
GEOMETRICAL HARMONICS AT R_{REF}=17 MM (10^{-4})

n	3	5	7	9	11
b_n	0.001	-0.009	0.117	0.263	-0.087

The calculated dependences of the sextupole field components b_3 produced by the persistent currents in superconducting filaments and the iron saturation vs. the magnet bore field are plotted in Fig. 5. The maximum absolute value of b_3 due to the persistent current effect is large ~ 23 units and it is reached at the bore field of ~1 T. In the BL design, it is more than a factor of 2 larger, ~48 units [4] for the same superconductor parameters. The b_3 variation due to the iron saturation is less than 12 units whereas in the BL design it was over 20 units [4]. The substantial reduction of both effects is a result of the more optimal turn distribution in the SM coil design.

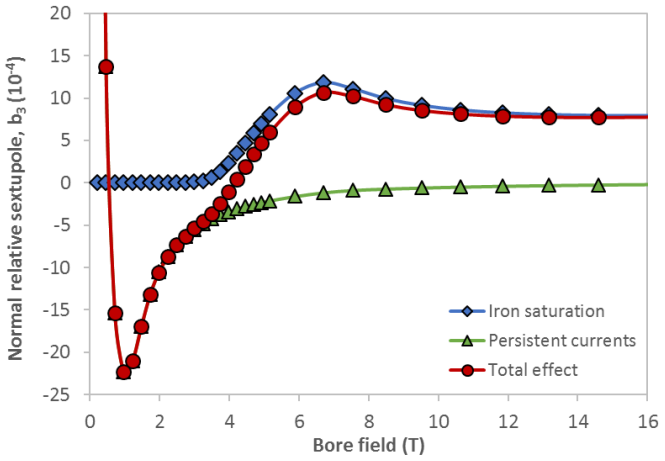

Fig. 5. Sextupole field component b_3 vs. the bore field.

IV. Mechanical Analysis

A. *FEA model and material properties*

A mechanical analysis of the described SM design was performed using ANSYS code and a simplified parametric model to evaluate displacements of key turns and stresses in the coil turns and in the coil SM structure. The material properties used in the analysis are summarized in Table 3.

TABLE III
MATERIAL PROPERTIES.

Structural element	Material	Thermal contract. (300-2 K), mm/m	Elasticity modulus, GPa
Coil (radial/azimuthal)	Nb_3Sn composite	2.9/3.3	40/40
Inner coil pole blocks	Ti-6Al-4V	1.7	125
Outer coil structure	St Steel	2.9	215
Inner coil wedges	Ti-6Al-4V	3.2	120
Coil-yoke spacer	St Steel	2.9	210
Yoke	Iron	2.0	225

The inner coil included Ti poles and wedges. The outer coil is integrated into the stainless steel structure which consists of half-cylinders with radial ribs in both layers.

The coil blocks were allowed to separate from the spacers and the structure to capture the effect of unloading under the Lorentz forces. In addition, each layer could slide with respect to the adjacent layers and to the iron yoke. It was also assumed that the vertical gap in the iron yoke remains closed at all fields. This condition must be provided by an appropriate mechanical structure. The coils were pre-compressed during the assembly by placing the appropriate radial shims between the inner and outer coils and between the outer coil and the iron yoke.

B. *Stresses and gaps*

Distributions of the equivalent stress in the coil after the cool-down and at the 17 T bore field are shown in Fig. 6. The peak equivalent stress without current is in layer 1 pole blocks and reaches 183 MPa. At the bore field of 17 T it moves to layer 4 midplane block (low field region) and approaches 185 MPa. It is lower than the peak stress in the inner-coil of the BL design at 15 T which is located in the layer 1 midplane block and reaches180 MPa.

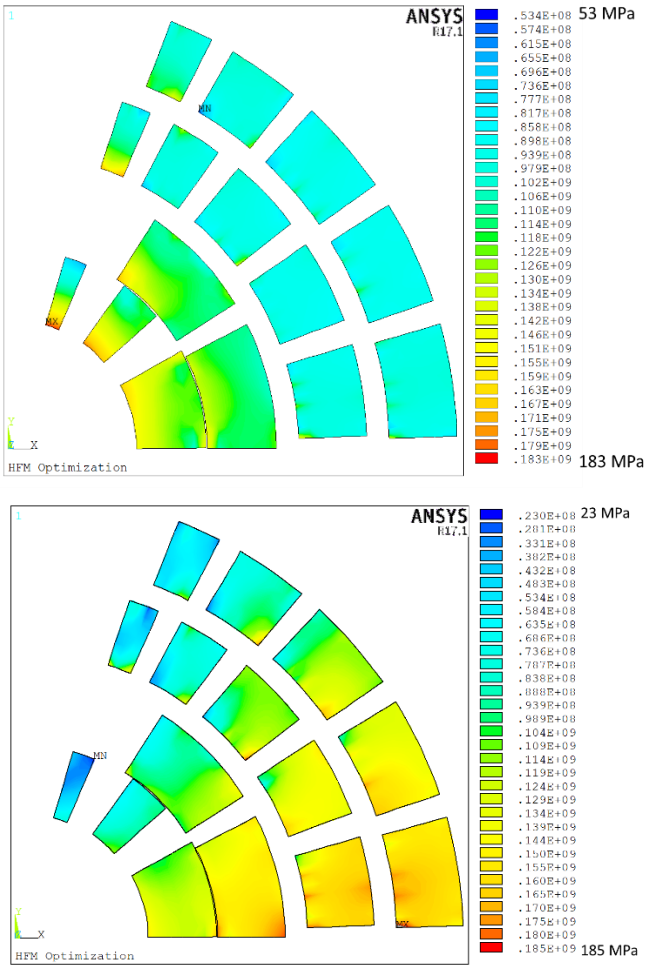

Fig. 6. The coil equivalent stress after cool-down (top) and at the bore field of 17 T (bottom).

The calculated gaps between the pole turns and the pole blocks in layers 1 and 2, and between the turns and the structure

in layers 3 and 4 at the bore field of 17 T are shown in Fig. 7. The inner coil pole turns remain in contact with the pole blocks at bore fields up to 17 T whereas in the BL design the layer 1 pole turn starts separating from the pole block at fields above 15 T. At 16 T, the gap reaches ~20 μm.

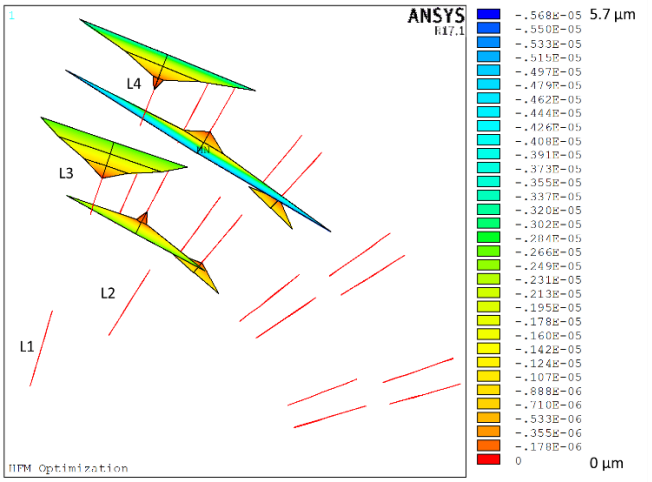

Fig. 7. Gaps between the pole turns and poles in layers 1 and 2, and between the turns and the structure in layers 3 and 4 at the bore field of 17 T.

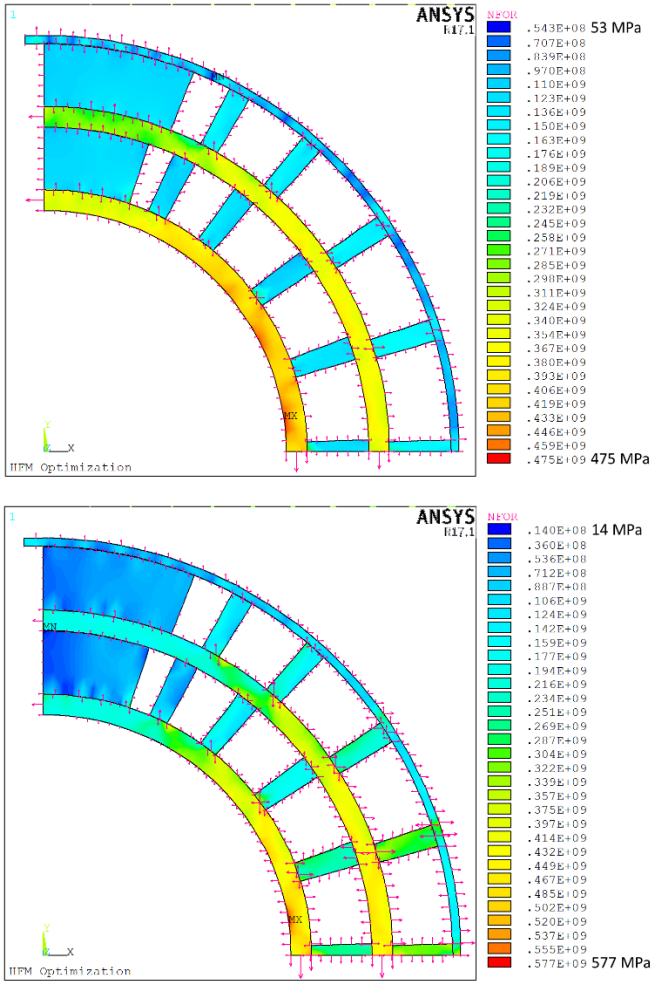

Fig. 8. Equivalent stress (Pa) in the outer coil structure after cooling-down (top) and at the bore field of 17 T (bottom).

In the three pole blocks of layer 3 and layer 4 partial gaps are seen on some rib-coil block interfaces. However, the maximum value of these partial gaps is less than 5 μm. Moreover, the gap length is less than the cable half-width which is considered acceptable.

Calculated distributions of the equivalent stress in the outer coil structure after cooling-down and at the bore field of 17 T are shown in Fig. 8. The peak equivalent stress in the support structure of the outer coil at the 17 T bore field is less than 600 MPa. This level of stress requires using special stainless steel grade, e.g. Nitronic-40 or similar, for this structural element. It can be also reduced by slightly increasing the radial thickness of the layer 3 spacer.

V. Conclusion

A Nb_3Sn dipole magnet based on a shell-type (aka cos-theta) coil with stress management has been developed and analyzed. Magnet design consists of a 4-layer graded cos-theta coil with 60-mm aperture and a cold iron yoke. Thanks to the larger number of turns the SM design reaches a higher maximum field in the aperture than the BL design [4]. The magnet maximum bore field estimated based on the state-of-the-art Nb_3Sn composite wires is ~16 T at 4.5 K and ~17.5 T at 1.9 K.

The coil geometry was optimized to reduce the level of Lorentz forces in layers 1 and 2. The SM structure was used in layers 3 and 4 to reduce large coil deformations under the Lorentz forces and, thus, the excessively high stresses in the coil and a separation of pole turns in layer 1 and 2 at high fields. It was shown that the SM design allows keeping the stresses in the coil and support structure within acceptable limits up to 17 T in the magnet bore.

There are large non-linear superconductor magnetization and iron saturation effects in the sextupole field component. However, with the same conductor parameters and iron properties these effects are a factor of two smaller in the SM design than in the BL design due to the more optimal turn distribution.

References

[1] L. Bottura et al., "Advanced Accelerator Magnets for Upgrading the LHC," IEEE Trans. on Appl. Supercond., v. 22, Issue 3, June 2012, 4002008.

[2] G. Ambrosio, "Nb3Sn High Field Magnets for the High-Luminosity LHC Upgrade Project," IEEE Trans. on Appl. Supercond., v. 25, Issue 3, June 2015, 4002107.

[3] Future Circular Collider Study Kickoff Meeting, Geneva, Switzerland, Feb. 12–14, 2014, https://indico.cern.ch/event/282344/

[4] I. Novitski et al., "Development of a 15 T Nb3Sn Accelerator Dipole Demonstrator at Fermilab," IEEE Trans. on Appl. Su-percond., v. 26, Issue 4, June 2016, 4001007.

[5] V.V. Kashikhin, I. Novitski, A.V. Zlobin, "Design studies and optimization of a high-field dipole for a future Very High Energy *pp* Collider", Proc. of IPAC2017, Copenhagen, Denmark, May 2017, p.3597.

[6] T. Elliott et al., "16 Tesla Nb3Sn Dipole Development at Texas A&M University," IEEE Trans. on Appl. Supercond., v. 7, Issue 2, June 1997, p. 555.

[7] S. Caspi et al., "Canted-Cosine-Theta Magnet (CCT) – A Concept for High Field Accelerator Magnets," IEEE Trans. on Appl. Supercond., v. 24, Issue 3, June 2014, 4001804.

[8] ROXIE code for an electromagnetic simulation and optimization of accelerator magnets, http://cern.ch/roxie.